U–Pb laser ablation ICP-MS zircon dating across the Ediacaran–Cambrian transition of the Montagne Noire, southern France

Maxime Padel, José Javier Álvaro, Sébastien Clausen, François Guillot, Marc Poujol, Martim Chichorro, Eric Monceret, M. Francisco Peirera, Daniel Vizcaïno

C. R. Geoscience xxx (2017) xxx–xxx

Contents lists available at ScienceDirect

Comptes Rendus Geoscience

www.sciencedirect.com

Petrology, Geochemistry (Geochronology)

U–Pb laser ablation ICP-MS zircon dating across the Ediacaran–Cambrian transition of the Montagne Noire, southern France

Maxime Padel [a,*], J. Javier Álvaro [b], Sébastien Clausen [a], François Guillot [c], Marc Poujol [d], Martim Chichorro [e], Éric Monceret [f], M. Francisco Pereira [g], Daniel Vizcaïno [h]

[a] UMR 8198 EEP CNRS, université de Lille-1, bâtiment SN5, avenue Paul-Langevin, 59655 Villeneuve-d'Ascq cedex, France
[b] Instituto de Geociencias (CSIC-UCM), Novais 12, 28040 Madrid, Spain
[c] UMR 8187 LOG CNRS, université de Lille–université du Littoral Côte d'Opale, SN5 Sciences de la Terre, 59655 Villeneuve-d'Ascq cedex, France
[d] Géosciences Rennes, UMR 6118, université de Rennes-1, campus de Beaulieu, 35042 Rennes, France
[e] GEOBITEC/Departamento de Ciências da Terra, Universidade Nova de Lisboa, Portugal
[f] 18, rue des Pins, 11570 Cazilhac, France
[g] IDL/Departamento de Geociências, ECT, Universidade de Évora, Portugal
[h] 7 c/o Jean-Baptiste Chardin, Maquens, 11090 Carcassonne, France

A R T I C L E I N F O

Article history:
Received 28 July 2016
Accepted after revision 25 November 2016
Available online xxx

Handled by Marc Chaussidon

Keywords:
Ediacaran
Cambrian
U–Pb dating
Montagne Noire

A B S T R A C T

U–Pb laser ablation inductively coupled plasma mass spectrometry was used for dating zircon grains extracted from four sedimentary and volcano sedimentary rocks of the Montagne Noire encompassing the presumed Ediacaran–Cambrian boundary interval. Magmatic zircon from two samples from the basal and middle parts of the Rivernous Formation (a rhyolitic tuff) were deposited at 542.5 ± 1 Ma and 537.1 ± 2.5 Ma, bracketing the 541 Ma age presently admitted as being at the Ediacaran–Cambrian boundary. In addition, a piece of sandstone from the underlying Rivernous Formation containing mostly euhedral zircon grains, suggesting proximal magmatic sources, yields Neoproterozoic dates ranging from 574 Ma to 1 Ga, and subsidiary older dates from 1.25 to 2.75 Ga. Another piece of sandstone from the overlying Marcory Formation yielded mostly rounded zircon grains probably issued from more remote areas, with a large spectrum dominated by Neoproterozoic dates as well as older ages up to 3.2 Ga. A comparison of both kinds of sandstone suggests a significant change in provenance, changing from a restricted source area during the Ediacaran to a much larger source domain during the Cambrian Epoch 2 that recorded contributions from different cratons of Gondwana.

* Corresponding author.
E-mail addresses: maxime.padel@etudiant.univ-lille1.fr (M. Padel), jj.alvaro@csic.es (J.J. Álvaro), sebastien.clausen@univ-lille1.fr (S. Clausen), Francois.Guillot@univ-lille1.fr (F. Guillot), marc.poujol@univ-rennes1.fr (M. Poujol), ma.chichorro@fct.unl.pt (M. Chichorro), eric.monceret@orange.fr (É. Monceret), mpereira@uevora.pt (M.F. Pereira), daniel.vizcaino@wanadoo.fr (D. Vizcaïno).

http://dx.doi.org/10.1016/j.crte.2016.11.002

1. Introduction

The pre-Variscan succession of the Montagne Noire crops out as a fold-and-thrust complex divided into two sedimentary-dominated, northern and southern flanks fringing an essentially metamorphic, Axial Zone (Arthaud, 1970; Gèze, 1949). Several tectonic models have been proposed for the Montagne Noire and are still subject of debate (Brun and Van Den Driessche, 1994; Charles et al., 2009; Faure and Cottereau, 1988; Fréville et al., 2016; Mattauer et al., 1996; Poujol et al., in press; Soula et al., 2001; Van Den Driessche and Brun, 1992). The Precambrian–Cambrian boundary has traditionally been tentatively located in the lowermost formation exposed in the southern Montagne Noire, namely the Marcory Formation (Álvaro et al., 1998). However, recent reviews of the northern successions challenged the former stratigraphic chart (Álvaro et al., 2014b; Devaere et al., 2013) and established a lower stratigraphic position for the volcano-sedimentary successions of the Grandmont, Rivernous and Layrac formations, exclusively exposed in the northern Montagne Noire. The only previous radiometric data from the Rivernous Formation (Fm.) yielded an Ordovician age, ranging from 473 ± 19 Ma to 443 ± 40 (Rb/Sr method; Demange, 1982), which was subsequently ruled out by biostratigraphic ages yielded by acritarch-bearing, laterally equivalent deposits (the so-called "Schistes X") from the Axial Zone (Fournier-Vinas and Debat, 1970). There, the "Schistes X" are capped by the Sériès Tuff ("Sériès" is a village name) tentatively correlated with the Rivernous Fm. The Sériès Tuff was dated at 545 ± 15 Ma by Pb-evaporation on zircon from a metadacite (Lescuyer and Cocherie, 1992). Some scarce zircon crystals were sampled in a garnet-grade Cambrian meta-siltstone from the southern Montagne Noire, giving a maximum depositional age of 556 Ma based only on a single zircon (Gebauer et al., 1989). This age attribution may look disputable, given the more recent statistical guidelines for provenance studies (see below) and also taking into account the marked metamorphic character of this rock. In fact, in a previous paper, Gebauer and Grünenfelder (1977) admitted that about 80% of the primitive radiogenic Pb might have been lost due to Phanerozoic thermal events. In order to improve the stratigraphic framework of the Neoproterozoic–Cambrian boundary interval, and the lithostratigraphic nomenclatural links between the Axial Zone and the northern and southern flanks of the Montagne Noire, zircon grains were sampled from the Rivernous, Grandmont and Marcory formations and dated by *in situ* LA-ICP-MS U–Pb analysis. Our results place new constraints upon the palaeogeographic affinities of the different tectonostratigraphic units that form the Montagne Noire, as well as on the detrital provenance of the Ediacaran–Cambrian sediments preserved in neighbouring tectonostratigraphic areas.

2. Geological and stratigraphic setting

Located in the southern part of the French Massif Central (Fig. 1A), the Montagne Noire represents a segment of the external, southwestern component of the Variscan Belt in Europe (Demange, 1998; Poujol et al., in press; Roger et al., 2004). As summarized above, this ENE–WSW-striking range is divided into three tectonic units: a central metamorphic dome, the so-called Axial Zone, fringed by its northern and southern flanks (Demange, 1985; Gèze, 1949).

The Axial Zone is essentially composed of micaschist, minor marble, paragneiss and migmatized orthogneiss (Gèze, 1949). The protolith age of the orthogneiss and its relationship with the metasedimentary rocks have been disputed. Some authors interpreted the orthogneiss as a granitic Precambrian basement (Demange, 1975, 1998), whereas others considered it as Palaeozoic intrusions (Bard and Loueyit, 1978). Recent conventional (ID-TIMS), SHRIMP and LA-ICP-MS U–Pb datings of various orthogneiss samples (Cocherie et al., 2005; Pitra et al., 2012; Roger et al., 2004) suggest that the granitic protolith was emplaced during the Ordovician.

The southern and northern sedimentary-dominated flanks of the Axial Zone are a fold-and-thrust complex of nappes (Fig. 1). The Precambrian–Cambrian boundary interval, only reported in the northern Montagne Noire (Álvaro et al., 2014b), comprises four formations, from bottom to top, the Grandmont, Rivernous, Layrac and Marcou formations (Fig. 2). The Grandmont Fm., about 700 m thick, consists of grey to black shales with subsidiary sandstone interbeds (Fig. 2). The Rivernous Fm., up to 200 m thick, comprises slightly metamorphosed rhyolitic tuffs that include rare breccia and shale interbeds (Fig. 2). Both formations crop out in the Avène–Mendic parautochthon, which includes the Lodévois inlier and the Lacaune thrust slice (Murat, Fig. 1B). In the Lacaune unit, a lateral equivalent of the Rivernous Fm. (locally named Murat Fm.), with base and top truncated by faults, was dated at 532 ± 12 Ma (U–Pb on zircon; Demange et al., 1995; Ducrot et al., 1979). In the Avène–Mendic parautochthon (Fig. 1), the rhyolitic palaeorelief formed by the Rivernous Fm. (up to about 300 m high, after Álvaro et al., 2014b) is unconformably onlapped by the volcano sedimentary conglomerates and sandstones of the Layrac Fm. (Fig. 2). The Layrac Fm. is itself overlain by the carbonate-dominated Marcou Fm., about 400 m thick and assigned to the Cambrian Stage 2 by recent biostratigraphic studies (Fig. 2, Devaere et al., 2013).

The above-reported formations are not exposed in the southern Montagne Noire, where the oldest outcrop is represented by the up to 1000 m-thick Marcory Fm. (Fig. 2), a monotonous alternation of sandstones and shales with subordinate carbonate nodules and layers. The upper part of the Marcory Fm. has been assigned to the Cambrian Stage 2–3 transition due to the occurrence of the ichnogenera *Psammichnites* and *Taphrelmintopsis* (Álvaro and Vizcaïno, 1999), and the oldest trilobites found in the Montagne Noire, i.e. *Blayacina miqueli* (Cobbold, 1935; Geyer, 1992). The Marcory Fm., although absent in the Avène–Mendic parautochthon, is exposed in other thrust slices and nappes of the northern Montagne Noire.

3. Material and methods

3.1. Material

The Grandmont and Rivernous Formations have been sampled at their stratotype, along the Rivernous rivulet

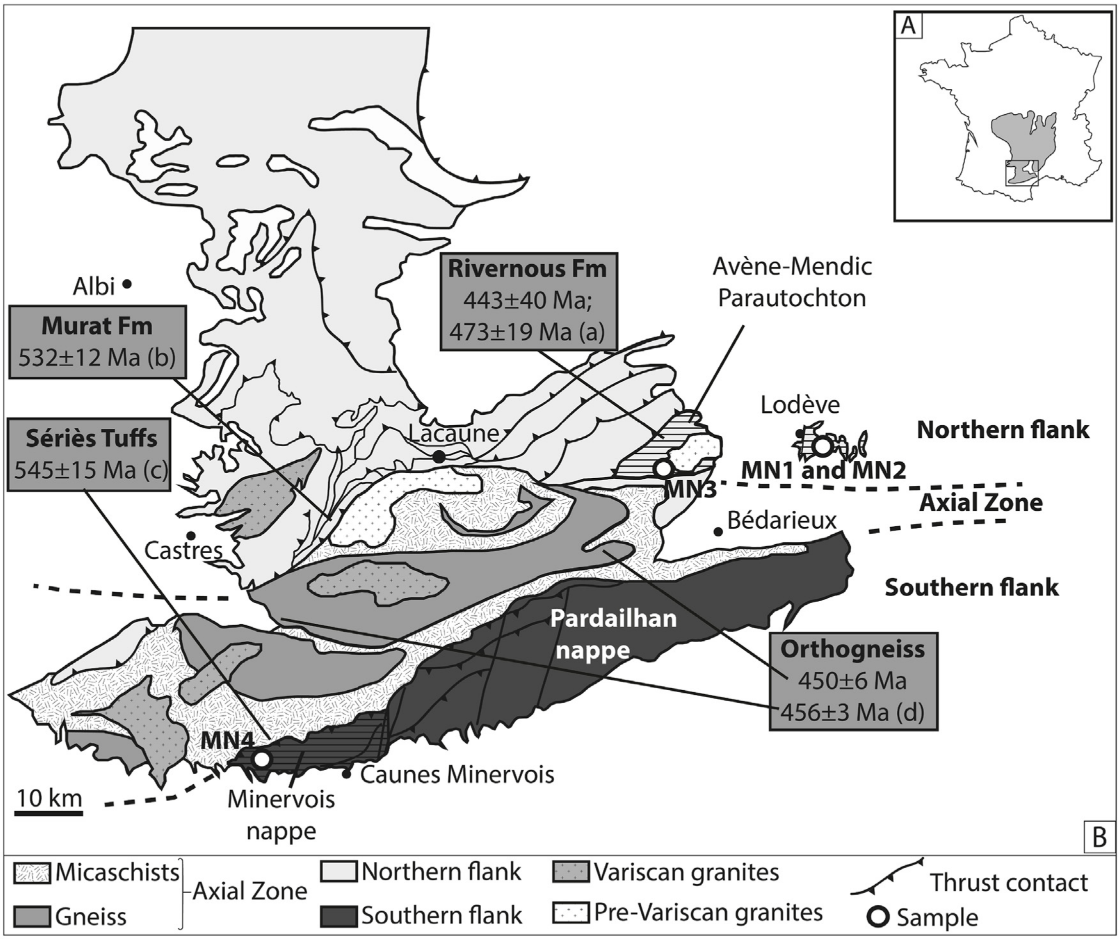

Fig. 1. Simplified geological map of the Montagne Noire; modified from Devaere et al. (2014). A, Location of the French Massif Central (grey) and Montagne Noire (rectangle) in France. B, Structural units and previous radiometric ages (a) Demange, 1982 (Rb/Sr) discarded by our results (see text); (b) Ducrot et al., 1979 (U–Pb) in Demange et al., 1995; and (c) Lescuyer and Cocherie, 1992 (U–Pb).

(about 4 km to the east of Lodève): a sandstone from the base of the exposed Grandmont Fm. (sample MN1), and a rhyolitic tuff from the base of the Rivernous Fm. (sample MN2). The Rivernous Fm. was also sampled at its middle part near the Col du Layrac (sample MN3). MN1 to MN3 samples belong to the so-called Avène–Mendic parautochthon. In order to investigate the provenance of the Marcory Fm., a sandstone (sample MN4) was also selected from the *Psammichnites gigas*-bearing level in the southern Montagne Noire (Álvaro and Vizcaïno, 1999), along the Orbiel river section of the Minervois nappe (Fig. 1).

3.2. Samples preparation

Zircon separation from fresh samples started with rock grinding using a steel crusher. The resulting powders were sieved in the range of 50–250 μm. Grains were separated first using a heavy liquid (sodium heteropolytungstates, density 2.85 g·cm^{-3}), then using a Frantz magnetic separator. Following Sláma and Košler (2012), the selected grains were obtained from random handpicking under a binocular microscope whatever their size, shape, or color, in order to avoid any operator bias. They were finally set in an epoxy resin puck and polished to expose their core

3.3. LA-ICP-MS in situ U–Pb dating

To identify internal growth textures and morphologies, zircon grains were imaged by scanning electron microscopy (SEM) to get cathodoluminescence and back-scattered electron images (at the "Laboratoire d'océanologie et de géosciences", University of Lille, France). The U–Pb ages of zircons were determined in situ at the Géosciences Rennes laboratory by LA-ICP-MS using an ICP-MS Agilent 7700x coupled with an ESI laser Excimer system producing a radiation with a wavelength of 193 nm (NWR193UC), with ablation spot diameters of 25 μm, energy pulses of 7J·cm^{-2}, and repetition rates of 5 Hz. Ablations were operated on both grain rims and cores. Where necessary, distinct domains of a zircon grain were analyzed to compare their ages. The resulting ablated material was mixed in a He, N and Ar gas mixture before being transferred into the plasma source of the ICP-MS device. Each analysis lasted 80 s and consisted of a first ∼20-s background measurement

Please cite this article in press as: Padel M, et al. U–Pb laser ablation ICP-MS zircon dating across the Ediacaran–Cambrian transition of the Montagne Noire, southern France. C. R. Geoscience (2017), http://dx.doi.org/10.1016/j.crte.2016.11.002

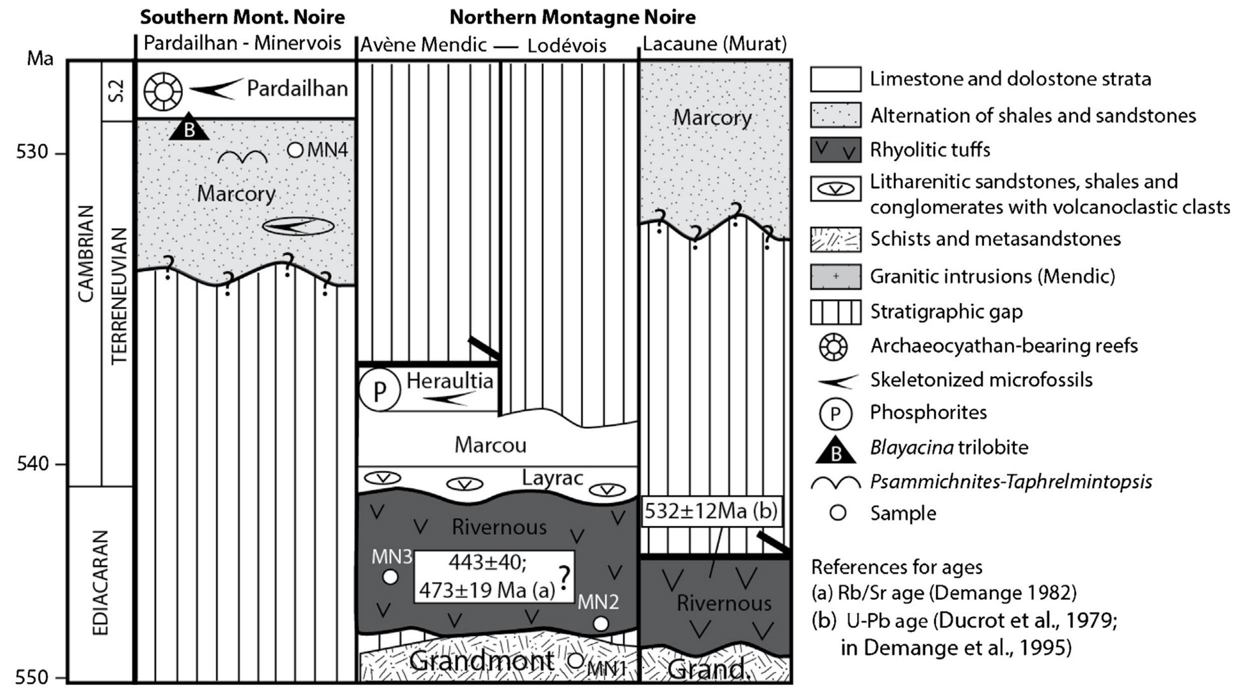

Fig. 2. Upper Ediacaran–lower Cambrian stratigraphic chart of the southern and northern Montagne Noire; modified from Álvaro et al. (2014b).

followed by ~60-s ablation with measurements of ^{204}(Hg + Pb), ^{206}Pb, ^{207}Pb, ^{208}Pb, ^{232}Th, and ^{238}U, and a ~15 s wash-out delay before the next acquisition. The data were collected in batch of 43 analyses divided in three sets of 10 unknowns, bracketed by two measurements of the GJ-1 primary zircon standard (Jackson et al., 2004) to correct for U–Pb and Th–Pb laser-induced fractionation and for instrumental mass discrimination, followed by one analysis of the Plesovice secondary zircon standard (Sláma et al., 2008) in order to check the precision and accuracy of the measurements. During the course of this study, the Plesovice zircon standard yielded a Concordia age of 336.8 ± 0.67 Ma (N = 32). The operating conditions for the LA-ICP-MS equipment can be found in Supplementary Table 1. For more information on the acquisition protocol, see Manzotti et al. (2015). Data treatment was performed with the GLITTER software (Van Achterbergh et al., 2001) and plotted using the Isoplot 3.75 software (Ludwig, 2012) in both Wetherill and Tera-Wasserburg Concordia diagrams. For rhyolitic tuffs, the ages were calculated using the TuffZirc Age algorithm (Ludwig and Mundil, 2002) together with the Sambridge and Compston (1994) algorithm. For the sandstones, age distribution curves with probability density plot were obtained using the density plotter freeware proposed by Vermeesch (2004). For dates > 1 Ga, we reported the ^{207}Pb/^{206}Pb dates and for ages < 1 Ga, we used the ^{206}Pb/^{238}U dates. The analyses out of the [90–110%] concordance interval, calculated with 100 × (^{207}Pb/^{235}U age)/(^{207}Pb/^{206}Pb age) for ages > 1 Ga (Meinhold et al., 2011) and 100 × (^{206}Pb/^{238}U age)/(^{207}Pb/^{235}U age) for ages < 1 Ga, were rejected (Faure and Mensing, 2005 and Talavera et al., 2012). The age of the youngest zircon population is derived from a cluster of at least three analyses from three different grains overlapping in age at 2σ (standard deviation), as proposed by Dickinson and Gehrels (2009) to ensure a statistically robust estimate of the maximum depositional ages. Percentages of concordance, isotopic ratios and ages with 1σ errors, as well as U and Pb concentrations are provided in Supplementary Table 2. In sedimentary rock samples (MN1 and MN4), about 110 grains were analyzed in order to get the best representation of the detrital zircon populations. For tuffs (MN2 and MN3), about 50 grains were analyzed, following the suggestions of Bowring et al. (2006), to give a robust estimate of the best age for the related volcanic event(s).

4. Results

4.1. Grandmont Formation (MN1)

Zircons from the sample MN1, medium-grained sandstone, are mostly in the 100–250 μm range, euhedral, facetted, rarely sub-rounded, colourless and generally well zoned (Supplementary data, Fig. S1). 107 of the 114 MN1 analyses were concordant [90–110%], among which 94% are Neoproterozoic (101 grains), 3% Mesoproterozoic (3 grains), 2% Paleoproterozoic (2 grains) and 1 grain (1%) is Archean in age (Fig. 4B). In the interval ranging from 500 to 1100 Ma, the probability curve shows a dominant Ediacaran group within the cluster 550–850 Ma, which displays a main peak around 605 Ma and a secondary one around 635 Ma (Fig. 4B). In this same cluster, four subsidiary peaks are identified around 690 Ma, 760 Ma, 805 Ma and 835 Ma. The Tonian-aged zircon grains are characterized by one peak around 906 Ma, in an 890–920 Ma cluster and another peak around 1 Ga in the 950–1050 Ma cluster. The four youngest and concordant zircon grains from this group ranging from 567.2 ± 6.12 Ma to

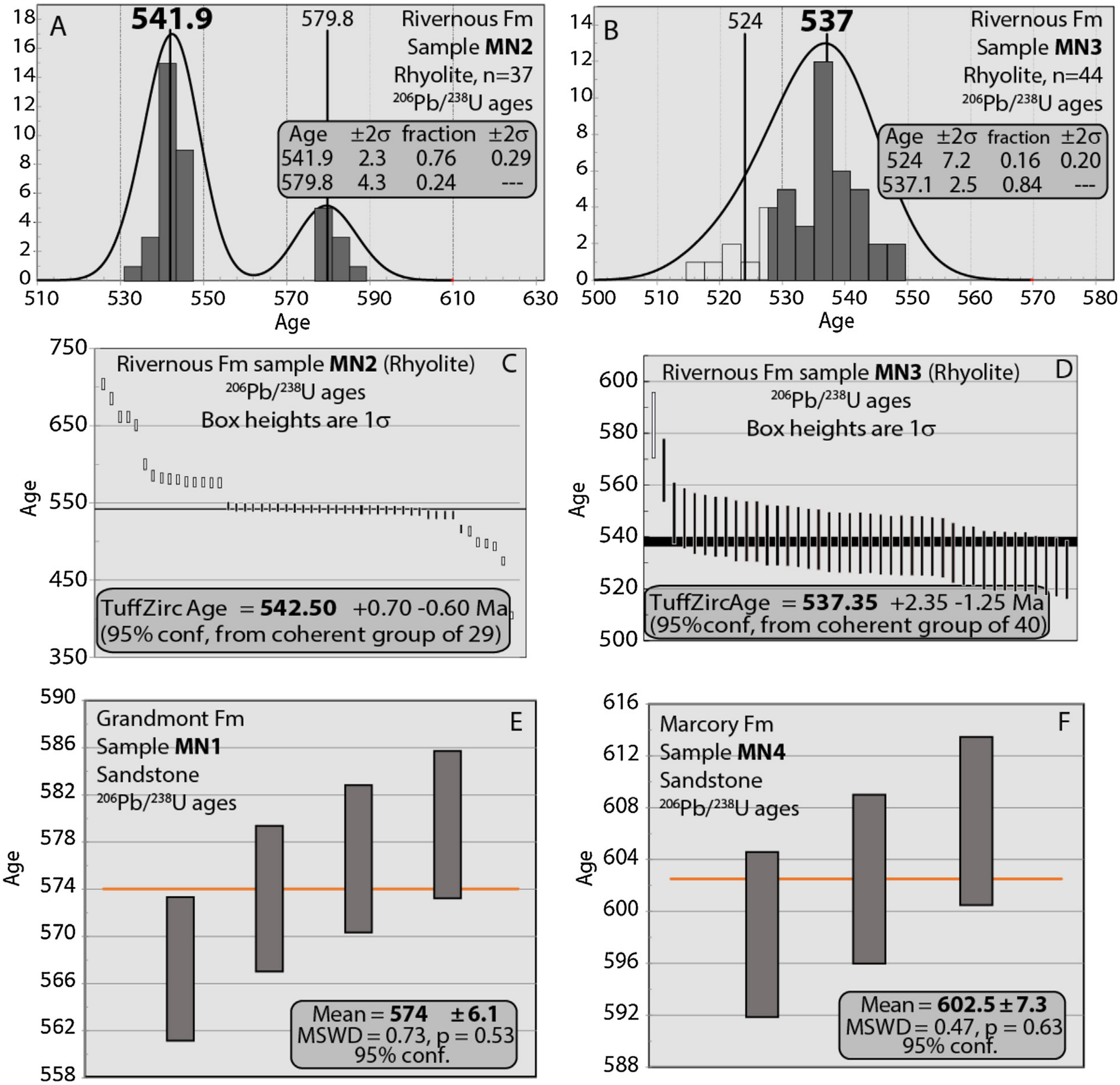

Fig. 3. LA-ICP-MS results for all samples using $^{206}Pb/^{238}U$ ages. Diagram A: mixture analysis for sample MN2 using Sambridge and Compston's (1994) approach; the age 579.8 ± 4.3 Ma is considered as inherited age. Diagram B: mixture analysis for sample MN3 using Sambridge and Compston (1994) approach; the age 524 ± 7.2 Ma is considered as geologically meaningless, due to lead loss. Diagrams C and D: data point age distribution for samples MN2 and MN3, resp., using TuffZirc Age (Ludwig and Mundil, 2002); chosen emplacement age for the rhyolitic tuffs of the Rivernous Fm. are: 542 ± 3 Ma (2σ) for sample MN2 and 537 ± 3 Ma (2σ) for sample MN3. Diagrams E and F: average age calculated for the youngest concordant zircon population of Grandmont and Marcory Fm. (sample MN1 and MN4), derived from a cluster of at least three analyses from three different grains overlapping in age at 2σ (standard deviation) as proposed by Dickinson and Gehrels (2009).

579.5 ± 6.28 Ma, yield an average date of 574 ± 6 Ma (95% conf., Fig. 3E).

4.2. Rivernous Formation (MN2 and MN3)

Samples MN2 and MN3 are both rhyolitic tuffs. Accordingly, zircon grains from samples MN2 and MN3 are euhedral, clear and colourless. Rarely cored, internal structures highlighted by the CL-imaging show clear magmatic zoning (Supplementary data, Fig. S1).

In sample MN2, 59 zircon grains were analysed, among which 50 gave concordant dates [90–110% as defined above]. Seven of the 50 analyses were rejected due to possible lead loss. Thus the youngest and main population from this sample represent 65% of these 43 zircon grains with individual $^{206}Pb/^{238}U$ dates ranging from 534.8 ± 6.01 Ma to 546 ± 6.02 Ma. The second group represents 23% of the total population, and gives $^{206}Pb/^{238}U$ dates ranging from 576.9 ± 6.3 Ma to 600.8 ± 6.7 Ma (Fig. 3A). Finally, five inherited core grains were dated at

651.6 ± 7.2 Ma, 661.8 ± 7.1 Ma, 662 ± 37.1 Ma, 685.8 ± 7.6 Ma and 704.7 ± 7.6 Ma (Table 2).

Looking at the youngest population, the TuffZirc Age algorithm returned a date of 542.5 +0.7/−0.6 Ma, while the Sambridge and Compston algorithm yielded a comparable date of 541.9 ± 2.3 Ma (Fig. 3A and C). Therefore, choosing between those two within error identical results, we conclude that this rhyolitic tuff was emplaced 542.5 +0.7/−0.6 Ma.

In sample MN3, 58 zircon grains were analysed, among which 52 yielded concordant results [90–110%]: two composite grains with cores (Zr 1 and Zr 27) yielding U–Pb dates of 1837.7 ± 19.1 Ma and 583.1 ± 6.37 Ma respectively. The youngest zircon population suggested by the Sambridge and Compston approach for sample MN3 returned a date around 524 Ma (Fig. 3B), which is poorly constrained, by only one concordant zircon among seven somewhat discordant data points (on a Concordia plot). Therefore, this date is interpreted as geologically meaningless as it could be linked to a possible lead loss.

Keeping only a group comprising three concordant data points (grey bars in Fig. 3B), the TuffZirc Age algorithm yielded a date of 537.35 +2.35/−1.25 Ma while the Sambridge and Compston approach returned a comparable date of 537.1 ± 2.5 Ma. This second rhyolitic sample was therefore emplaced 537.1 ± 2.5 Ma ago (2σ) (Fig. 3B and D).

4.3. Marcory Formation (MN4)

Sample MN4 is a fine-grained and mature sandstone. Accordingly, its zircon crystals are mostly anhedral, rounded to subrounded, often broken and rarely bi-pyramidal, largely in the 50–100-μm size range. They are colourless to yellowish, though the biggest zircon grains are reddish in colour. In the analysed fraction, 104 of the 112 MN4 analyses were concordant [90–110%], among which 87% are Neoproterozoic (90 grains), 4% Mesoproterozoic (4 grains), 5% Paleoproterozoic (6 grains), 2% Neoarchean (2 grains), one grain is Mesoarchean and the oldest one is Paleoarchean in age at 3.2 Ga (Fig. 4A).

The probability density curve (Vermeesch, 2004) shows a dominant Ediacaran group (clustered across 550–850 Ma), with a main peak around 614 Ma and a secondary peak around 575 Ma (Fig. 4A). In this same cluster, six other peaks are identified around 651 Ma, 678 Ma, 700 Ma, 737 Ma, 800 Ma and 850 Ma. The Tonian-aged zircon grains are characterized by one peak around 900 Ma in an 890–920 Ma cluster and another distinctive peak around 1 Ga in the 950–1050 Ma cluster. The three youngest dates obtained from this sample that are concordant yield an average date of 602.5 ± 7.3 Ma (Fig. 3F).

5. Discussion

5.1. The Rivernous volcanic activity marking the Precambrian–Cambrian boundary interval

The two dates (537.1 ± 2.5 Ma and 542.5 +0.7/−0.6 Ma) obtained from the Rivernous rhyolitic tuffs are much older than previously estimated (473 ± 19 Ma and 443 ± 40 Ma; Demange, 1982). These results allow us to confidently identify the Precambrian–Cambrian boundary (541 Ma, Gradstein et al., 2012) in the basal succession of the Montagne Noire. By comparison with the previously determined age of the Sériès Tuffs from the Axial Zone (545 ± 15 Ma; Lescuyer and Cocherie, 1992) and the Rivernous (former Murat) Fm. in the Lacaune thrust slice of the northern flank (532 ± 12 Ma, intercept superior; Demange et al., 1995 and references therein; Figs. 1–2), these results support the lateral equivalence of the Sériès volcanic episode (Axial Zone) and Rivernous rhyolitic tuff deposition (northern flank), as already suggested (Pouclet et al., in press).

In other Variscan units of the Ibero-Armorican Arc, some plutonic bodies have recently been dated around 540 Ma by LA-ICPMS (Supplementary data, Fig. S2; see also Casas et al., 2015; Castiñeiras et al., 2008; Gutiérrez-Alonso et al., 2004; Melleton et al., 2010; Rubio-Ordóñez et al., 2015): the Arc-de-Fix and Ardéchois augen gneisses in the Massif Central, with respective Concordia age of 541.8 ± 3.1 and 542.5 ± 3.1 Ma (Couzinié et al., this issue), as well as the Laparan orthogneiss in the Central Pyrenees, with a Concordia age of 545 ± 3 Ma (Mezger and Gerdes, 2016). All these plutonic and volcanic events, overlapping in age within error, should be linked to a common episode associated with the voluminous magmatic and anatectic Cadomian events reported for West Gondwana, among others, by Linnemann et al. (2007, 2008). According to these authors, the numerous plutonic and volcanic to volcano sedimentary complexes identified in the Ossa-Morena, Saxo-Thuringian and Anti-Atlas zones (Álvaro et al., 2014a; Blein et al., 2014) can result from a slab breakoff of a southward subducted oceanic plate ending with the Cadomian cycle at about 545–540 Ma. The end of the Pan-African/Cadomian cycle led to the onset of a Cambrian magmatic cycle (Supplementary data, Fig. S2), related to the rifting of the North Gondwana margin (Álvaro et al., 2014a, 2014b; Pouclet et al., in press).

5.2. Age and potential provenances of the Grandmont and Marcory formations

Depositional ages. The youngest group of concordant zircon grains from the Grandmont Fm. (sample MN1) yield an average date of 574 ± 6 Ma that is interpreted here as its maximum depositional age (i.e. late Ediacaran; Fig. 3E). This result is coherent with the stratigraphic framework proposed by Álvaro et al. (2014b) and the Neoproterozoic age based on acritarchs reported from the "Schistes X" Fm. of the Axial Zone (Fournier-Vinas and Debat, 1970). As a result, this maximum age of deposition supports their correlation between the Grandmont and "Schistes X" formations (Álvaro et al., 2014b).

The average date calculated from the youngest group of concordant data for the Marcory Fm. at 602.5 ± 7.3 Ma (Fig. 3F) might be considered as a maximum depositional age. However, it is far from the real depositional age, as mentioned above. Indeed, this sample was selected from the *Psammichnites gigas*-bearing level (Fig. 2), and consequently must be assigned to the Cambrian Stage 2–3 transition, i.e. it is less than 521 Ma old.

Source of the pre-ca. 1 Ga detrital zircon grains. The age spectra obtained for the samples from the Marcory

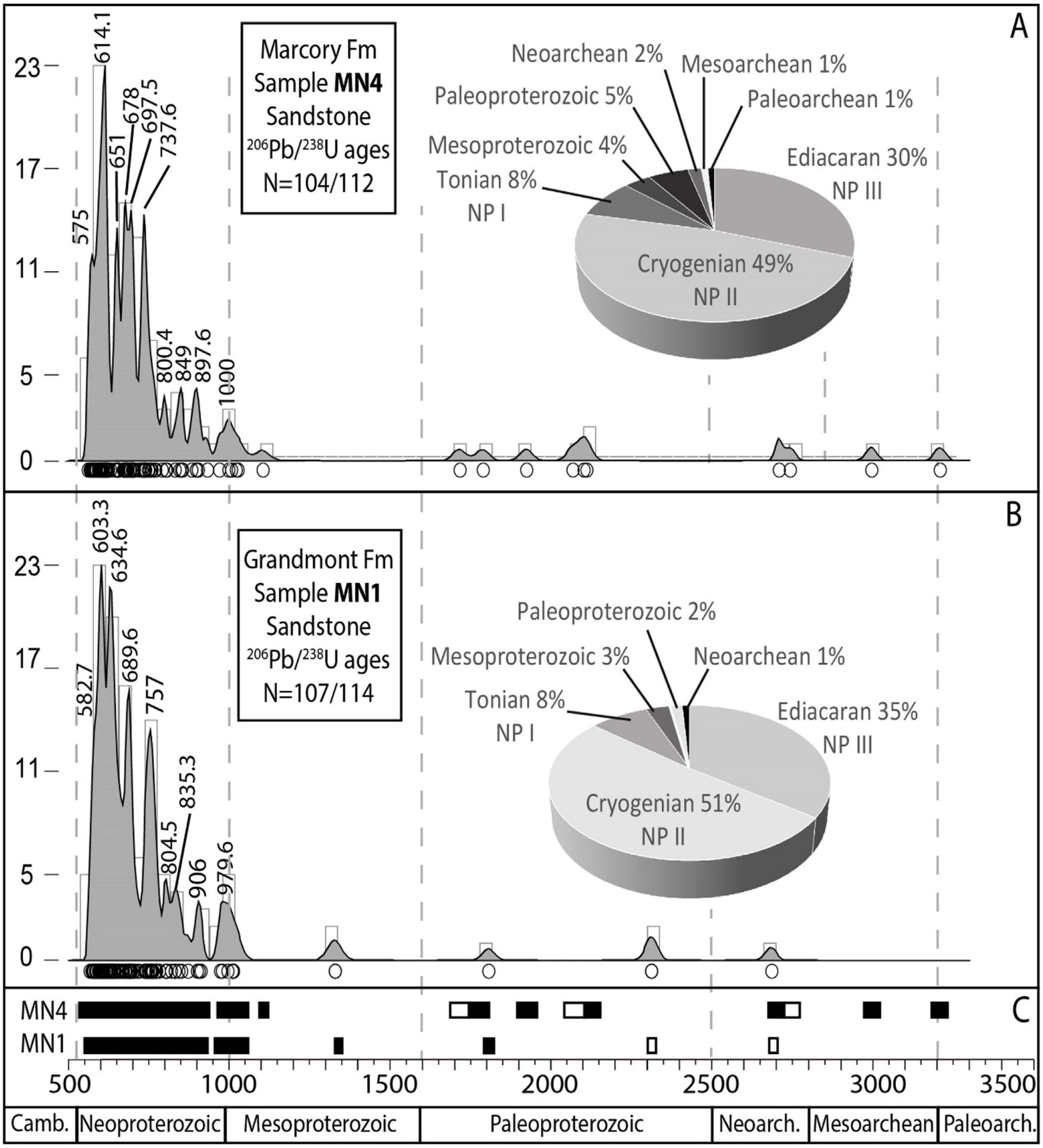

Fig. 4. Frequency and probability density plots of detrital zircon grains in the range 500–3300 Ma for samples MN1 (B) and MN4 (A). Age groups of each sample are presented in a pie diagram. Section C shows a comparison of age groups where white boxes represent dates from inherited core and black boxes relate to dates from zoned rims.

(MN4) and Grandmont (MN1) formations are somewhat similar, but display some differences. Although each individual singleton-date should be treated with caution, the distributions of pre-1 Ga ages are plainly distinct (Figs. 4 and 5).

As mentioned above, zircon grains from the Marcory Fm. (sample MN4) are much smaller and definitely more rounded (Supplementary data, Fig. S1) than those from the Grandmont Fm. (sample MN1), suggesting a long distance of transport for the former grains. We have separated data from inherited cores (white boxes in Fig. 4), meaningless regarding the source age, from data from zoned magmatic rims (black boxes, Fig. 4) that represent most probably the age of the source-rock. From this respect, the oldest zircon rim from the Grandmont Fm. (MN1) is only Late Paleoproterozoic (1806 ± 19 Ma), and only two grain rims are older than 1 Ga. By contrast, the presence of several Archean zircon rims in MN4 points to a major change in the source areas. MN1 zircon grains could possibly be derived, ultimately, from the Amazonian craton (Rhyacian, Orosirian and Statherian events), more probably from the Eburnean West African craton, or from the Saharan metacraton (Fig. 5). By contrast, eight pre-1Ga zircon rims from sample MN4 form a Paleoproterozoic group (cluster ranging from

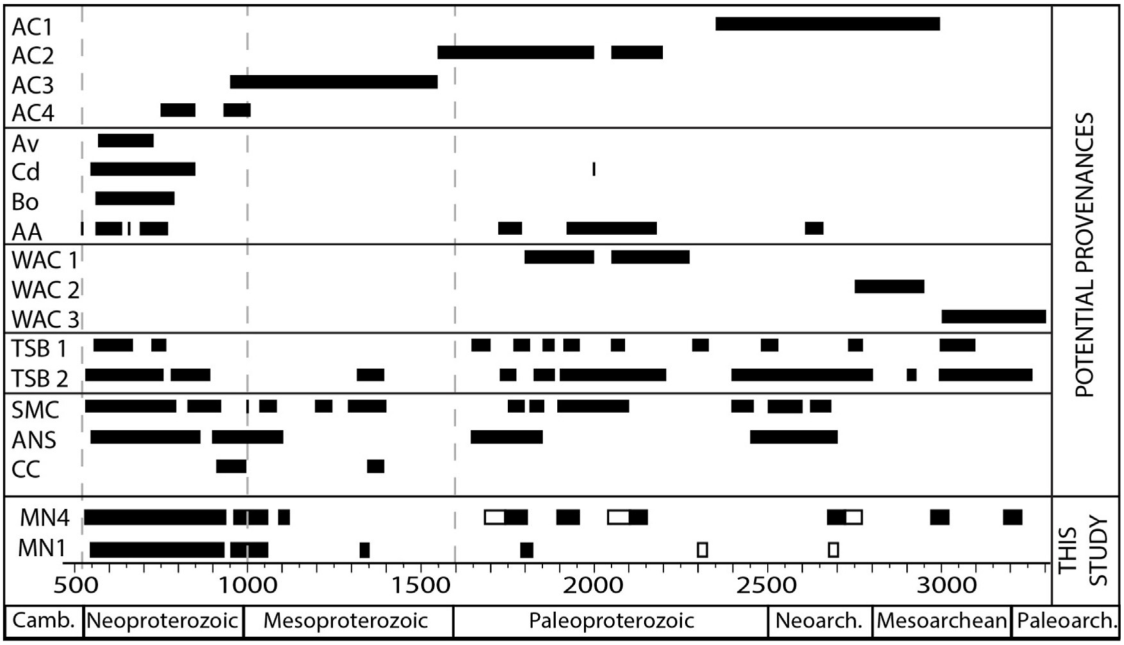

Fig. 5. Potential sources for samples MN1 and MN4 (modified after Drost et al., 2011; Linnemann et al., 2011; Pereira et al., 2011; Pereira et al., 2012; Tack et al., 2001; Tack et al., 2010). AC1: Siderian event of the Amazonian craton; AC2: Rhyacian, Orosirian and Statherian events of the Amazonian craton; AC3: San Ignacio and Sunsas events of the Amazonian craton; AC4: eastern margin of the Amazonian craton; Av: Avalonia; Cd: Cadomia; Bo: Bohemian massif; AA: Anti-Atlas; WAC1: Eburnean event of the West African craton; WAC2: Liberian event of the West African craton; WAC3: Leonan event of the West African craton; TSB1: Trans-Saharan belt, Benin-Nigerian shield; TSB2: Trans-Saharan belt, Tuareg shield; SMC: Saharan metacraton; ANS: Arabian–Nubian shield; CC: Congo craton.

2109 ± 19 Ma to 1787 ± 20 Ma) and an Archean group. Those groups fit much better with an African source comprising Eburnean areas plus Archean West African craton (Fig. 5).

However, we should not exclude that the availability of zircon to erosion and transport from either primary crystalline or recycled sources requires that the zircon-bearing rocks be exposed at the appropriate time, and recycling from older sedimentary deposits may constitute a more significant source than from primary crystalline rocks.

Sources of the Stenian–Tonian detrital zircons. The cluster pointing to the Stenian–Tonian transition (950 to 1100 Ma) in samples MN1 and MN4 could share a common origin (Fig. 4). One should expect an Amazonian craton affinity (Linnemann et al., 2011) with detrital sources related to the San Ignacio and Sunsas events and on its eastern margin (Pereira et al., 2012). However, many studies on sandstones from Lower Palaeozoic peri-Gondwanan exposures around the Mediterranean region (e.g., Israel, Jordan, Libya, Pyrenees, Sardinia, Greece and Sicily) rule out an Amazonian provenance and suggest instead an eastern to southeastern African origin (Altumi et al., 2013; Avigad et al., 2003; Avigad et al., 2012; Kydonakis et al., 2014; Margalef et al., in press; Meinhold et al., 2011; Meinhold et al., 2013; Williams et al., 2012). Therefore, the Arabian–Nubian shield, the Saharan metacraton, possibly the western edge of the Congo craton (Tack et al., 2001), as well as its eastern part recording the "Kibaran Event" (Tack et al., 2010) and the Irumide belt (Meinhold et al., 2011), fit well as potential sources for Mesoproterozoic and Stenian–Tonian zircon grains. These zircon-forming events occurred simultaneously with the assembly of the supercontinent Rodinia (Grenvillian orogeny). Different hypotheses have been advanced to explain this input of Mesoproterozoic and Stenian–Tonian zircon crystals (Altumi et al., 2013), including: (i) the transport of large amounts of sediment through Neoproterozoic glaciers following an original south–north transect, later reworked and deposited (Avigad et al., 2003); and (ii) a source region linked to the Transgondwanan supermountain range resulting from the East African–Antarctic Orogen and formed during the protracted Late Neoproterozoic docking of East and West Gondwana (Williams et al., 2012), involving the development of a super-fan system (Kydonakis et al., 2014; Squire et al., 2006).

Sources of Neoproterozoic detrital zircons. Neoproterozoic grains display similar age distributions in the Grandmont and Marcory formations: a main Neoproterozoic population of zircon grains (with one predominant Ediacaran group) followed by five similar peaks across the Tonian–Cryogenian interval (Fig. 4). Potential sources for these detrital zircons are located in the eastern (Saharan metacraton, Arabian-Nubian shield) and western (Trans-Saharan belt, Pan-African suture of the Anti-Atlas, early and late Cadomian arcs, and Avalonian Arc) area of the North-Gondwana margin (Fig. 5). The probability density curve of the Marcory Fm., as well as the shape and roundness of its zircon grains, implies more remote origins for them than for the Grandmont Fm. ones. Therefore, a comparison of the morphological and age differences of these zircon grains suggests an evolution of the depositional basin and it sourcing from a narrow basin being infilled by the Grandmont Fm., probably a back-arc basin resulting from the Panafrican/Cadomian orogeny, to a more evolved and opened basin infilled by the Marcory Formation, represents a more evolved and widespread basin with wider potential source areas, developed during the break-up of West Gondwana.

A composite zircon grain of the Grandmont sandstone (sample MN 1; ZR 49) demonstrates that crust with ca. 586 Ma old rocks became recycled during magmatism at ca. 567 Ma, and underlines the existence of two distinct Ediacaran magmatic events in the source area.

One should expect to identify the Ediacaran Rivernous volcanic event as reworked zircon grains in the overlying Cambrian Marcory Fm. However, this is not the case. A rapid burial of the Rivernous volcano sedimentary palaeorelief, related to high rates of sedimentation and available accommodation space due to active thermal subsidence, has been proposed for Furongian to Early Ordovician times in West Gondwana (Linnemann et al., 2011; Pereira et al., 2012) and the late Neoproterozoic–early Cambrian in the ANS (Avigad and Gvirtzman, 2009) or post-Cadomian rifting extension (Pouclet et al., in press; Von Raumer and Stampfli, 2008), which should preclude reworking of the Rivernous from distal (northern) to proximal areas (southern Montagne Noire).

6. Conclusions

The Ediacaran–Cambrian boundary has been confidently identified within error, based on U–Pb zircon dating, into the Rivernous Fm. of the northern Montagne Noire. The Rivernous volcanic event is indicated to be the lateral equivalent of the Sériès Tuff of the Axial Zone. This fits well with a latest Ediacaran depositional age (ca. 574 Ma) estimated with detrital zircon U–Pb geochronology for the underlying Grandmont Fm. The latter should be considered as a time-stratigraphic equivalent of the acritarch-bearing "Schist X" Fm. of the Axial Zone (Supplementary data, Fig. S3).

U–Pb analysis of the detrital zircons from the Ediacaran Grandmont Fm. and the Cambrian Series 2 Marcory Fm. suggests a change over time in the sourcing. The Ediacaran sediments were deposited in a narrow back-arc basin far from the influence of far cratonic sources, whereas Cambrian Series 2 detrital sediments were derived from mature source rocks involving the denudation of different Gondwanan cratons.

Acknowledgements

The authors thank constructive criticism made by O. Blein and B. Laumonier, and founding from the RGF program of the French Geological Survey (BRGM). This paper is a contribution to project CGL2013-48877-P from Spanish MINECO.

Appendix A. Supplementary data

Supplementary data associated with this article can be found, in the online version, at http://dx.doi.org/10.1016/j.crte.2016.11.002.

References

Altumi, M.M., Elicki, O., Linnemann, U., Hofmann, M., Sagawe, A., Gärtner, A., 2013. U–Pb LA-ICP-MS detrital zircon ages from the Cambrian of Al Qarqaf Arch, central-western Libya: Provenance of the West Gondwanan sand sea at the dawn of the Early Palaeozoic. J. Afr. Earth Sci. 79, 74–97.

Álvaro, J.J., Vizcaïno, D., 1999. Biostratigraphic significance and environmental setting of the trace fossil Psammichnites in the Lower Cambrian of the Montagne Noire (France). Bull. Soc. geol. France 170, 821–828.

Álvaro, J.J., Courjault-Radé, P., Chauvel, J.-J., Dabard, M.-P., Debrenne, F., Feist, R., Pillola, G.L., Vennin, E., Vizcaïno, D., 1998. Nouveau découpage stratigraphique des séries cambriennes des nappes de Pardailhan et du Minervois (versant sud de la Montagne noire, France). Geol. Fr. 1998 (2), 3–12.

Álvaro, J.J., Benziane, F., Thomas, R., Walsh, G.J., Yazidi, A., 2014a. Neoproterozoic–Cambrian stratigraphic framework of the Anti-Atlas and Ouzellagh promontory (High Atlas), Morocco. J. Afr. Earth Sci. 98, 1–15.

Álvaro, J.J., Baulus, B., Clausen, S., Devaere, L., Imaz, A.G., Monceret, E., Vizcaïno, D., 2014b. Sratigraphy of the Cambrian-Lower Ordovician volcano sedimentary complexes, northern Montagne Noire, France. Stratigraphy 11, 83–96.

Arthaud, F., 1970. Étude tectonique et microtectonique comparée de deux domaines hercyniens : les nappes de la Montagne noire (France) et l'anticlinorium de l'Iglesiente (Sardaigne). PhD, Université de Montpellier. Pub. USTELA, Montpellier. Ser Geol. Struct. 1, 175p.

Avigad, D., Gerde, A., Morag, N., Bechstädt, T., 2012. Coupled U–Pb–Hf of detrital zircons of Cambrian sandstones from Morocco and Sardinia: implications for provenance and Precambrian crustal evolution of North Africa. Gondwana Res. 21, 690–703.

Avigad, D., Gvirtzman, Z., 2009. Late Neoproterozoic rise and fall of the northern Arabian–Nubian shield: the role of lithospheric mantle delamination and sub-sequent thermal subsidence. Tectonophysics 477, 217–228.

Avigad, D., Kolodner, K., McWilliams, M., Persing, H.M., Weissbrod, T., 2003. Origin of northern Gondwana Cambrian sandstone as revealed by SHRIMP dating of detrital zircons. Geology 31, 227–230.

Bard, J.-P., Loueyit, G., 1978. Sur l'origine des gneiss oeillés de l'Espinouse dans la zone axiale de la Montagne noire (Massif central) ; conséquences tectoniques. Bull. Soc. geol. France 20, 751–772.

Blein, O., Baudin, T., Soulaimani, A., Cocherie, A., Chèvremont, P., Admou, H., Ouanaimi, H., Hafid, A., Razin, P., Bouadbelli, M., Roger, J., 2014. New geochemical, geochronological and structural constraints on the Ediacaran evolution of the South Sirwa, Agadir-Melloul and Iguerda inliers, Anti-Atlas, Morocco. J. Afr. Earth Sci. 98, 47–71.

Bowring, S.A., Schoene, B., Crowley, J.L., Ramezani, J., Conon, D.J., 2006. High-precision U–Pb zircon geochronology and the stratigraphic record: progress and promise. Geochronology: Emerging Opportunities, Paleontological Society Short Course. Paleontol. Soc. Pap. 11, 23–43.

Brun, J.-P., Van Den Driessche, J., 1994. Extensional gneiss dome and detachment fault systems: structure and kinematics. Bull. Soc. geol. France 165, 519–530.

Casas, J.M., Navidad, M., Castiñeiras, P., Liesa, M., Aguilar, C., Carreras, J., Hofmann, M., Gärtner, A., Linnemann, U., 2015. The Late Neoproterozoic magmatism in the Ediacaran series of the Eastern Pyrenees: new ages and isotope geochemistry. Int. J. Earth Sci. 104, 909–925.

Castiñeiras, P., Navidad, M., Liesa, M., Carreras, J., Casas, J.M., 2008. U–Pb zircon ages (SHRIMP) for Cadomian and Lower Ordovician magmatism in the Eastern Pyrenees: new insights in the pre-Variscan evolution of the northern Gondwana margin. Tectonophysics 461, 228–239.

Charles, N., Faure, M., Chen, Y., 2009. The Montagne Noire migmatitic dome emplacement (French Massif Central): new insights from petrofabric and AMS studies. J. Struct. Geol. 31, 1423–1440.

Cobbold, E.S., 1935. Lower Cambrian faunas from Hérault, France. Ann. Mag. Nat. Hist. (ser. O) 16, 25–48.

Cocherie, A., Baudin, T., Autran, A., Guerrot, C., Fanning, M., Laumonier, B., 2005. U–Pb zircon (ID-TIMS and SHRIMP) evidence for the early Ordovician intrusion of metagranites in the Late Proterozoic

Canaveilles Group of the Pyrenees and the Montagne Noire (France). Bull. Soc. geol. France 176, 269–282.
Couzinié, S., et al., 2017. C. R. Geoscience. 349 (this issue).
Demange, M., 1975. Style pennique de la zone axiale de la Montagne noire entre Saint-Pons et Murat-sur-Vèbre (Massif central). Bull. BRGM I (2), 91–139 (2e série).
Demange, M., 1982. Étude géologique du massif de l'Agout, Montagne noire (PhD, Université Paris-6). .
Demange, M., 1985. The eclogite-facies rocks of the Montagne Noire, France. Chem. Geol. 50, 173–188.
Demange, M., 1998. Contribution au problème de la formation des dômes de la zone axiale de la Montagne noire : analyse géométrique des plissements superposés dans les séries métasédimentaires de l'enveloppe. Implications pour tout modèle géodynamique. Geol. Fr. 4, 3–56.
Demange, M., Guérangé-Lozes, J., Guérangé, B., 1995. Notice explicative, Carte géologie France (1/50 000), feuille Lacaune (987). BRGM, Orléans (153 p.).
Devaere, L., Clausen, S., Steiner, M., Álvaro, J.J., Vachard, D., 2013. Chronostratigraphic and palaeogeographic significance of an Early Cambrian microfauna from the Heraultia Limestone, northern Montagne Noire, France. Palaeont. Electr. 16.2.17A, 755–768.
Dickinson, W.R., Gehrels, G.E., 2009. Use of U–Pb ages of detrital zircons to infer maximum depositional ages of strata: a test against a Colorado Plateau Mesozoic database. Earth Planet. Sci. Lett. 288, 115–125.
Drost, K., Gerdes, A., Jeffries, T., Linnemann, U., Storey, C., 2011. Provenance of Neoproterozoic and Early Paleozoic silicicastic rocks of the Tepla-Barrandian unit (Bohemian Massif): Evidence from U–Pb detrital zircon ages. Gondwana Res. 19, 213–231.
Ducrot, J., Lancelot, J.-R., Reille, J.-L., 1979. Datation en Montagne noire d'un témoin d'une phase majeure d'amincissement crustal caractéristique de l'Europe prévarisque. Bull. Soc. geol. France 21, 501–505.
Faure, M., Cottereau, N., 1988. Données cinématiques sur la mise en place du dôme migmatitique carbonifère moyen de la zone axiale de la Montagne noire (Massif central, France). C. R. Acad. Sci. Paris, Ser. II 307, 1787–1794.
Faure, G., Mensing, T.M., 2005. Isotopes: principles and applications. Wiley, Hoboken (897 p.).
Fournier-Vinas, C., Debat, P., 1970. Présence de micro-organismes dans les terrains métamorphiques précambriens (schistes X) de l'Ouest de la Montagne noire. Bull. Soc. geol. France 12, 351–355.
Fréville, K., Cenki-Tok, B., Trap, P., Rabin, M., Leyreloup, A., Régnier, J.-L., Whitney, D.L., 2016. Thermal interaction of middle and upper crust during gneiss dome formation: example from the Montagne Noire (French Massif Central). J. Metamorph. Geol. 34, 447–462.
Gebauer, D., Grünenfelder, M., 1977. U–Pb systematics of detrital zircons from some unmetamorphosed to slightly metamorphosed sediments of central Europe. Contrib. Mineral. Petrol. 65, 29–37.
Gebauer, D., Williams, I.S., Compston, W., Grünenfelder, M., 1989. The development of the Central European Continental crust since the Early Archaean based on conventional and ion-microprobe dating of up to 3.84 b.y. old detrital zircons. Tectonophysics 157, 81–96.
Geyer, G., 1992. A re-evaluation of Blayacina Cobbold, 1932 and Thoralaspis Hupé, 1953 (Trilobita: Redlichiida). Paleont. Z. 66, 99–113.
Gèze, B., 1949. Étude géologique de la Montagne noire et des Cévennes méridionales. Mem. Soc. geol. France 62, 1–215.
Gradstein, F.M., Ogg, J.G., Schmitz, M.D., Ogg, G.M. (Eds.), 2012. The geological time scale 2012, Elsevier, Amsterdam (2 vols, 1144 p.).
Gutiérrez-Alonso, G., Fernández-Suárez, J., Jeffries, T.E., 2004. Age and setting of the Upper Neoproterozoic Narcea Antiform volcanic rocks (NW Iberia). Geogaceta 35, 78–82.
Jackson, S.E., Pearson, N.J., Griffin, W.L., Belousova, E.A., 2004. The application of laser-ablation-inductively coupled plasma-mass spectrometry to in situ U–Pb zircon geochronology. Chem. Geol. 211, 47–69.
Kydonakis, K., Kostopoulos, D., Poujol, M., Brun, J.-P., Papanikolaou, D., Paquette, J.-L., 2014. The dispersal of the Gondwana Super-fan System in the eastern Mediterranean: new insights from detrital zircon geochronology. Gondwana Res. 25, 1230–1241.
Lescuyer, J.-L., Cocherie, A., 1992. Datation sur monozircons des metadacites de Sériès. Arguments pour un âge protérozoïque terminal des « schistes X » de la Montagne noire (Massif central français). C. R. Acad. Sci. Paris, Ser. II 314, 1071–1077.
Linnemann, U., Gerdes, A., Drost, K., Buschmann, B., 2007. The continuum between Cadomian Orogenesis and opening of the Rheic Ocean: constraints from LA-ICP-MS U–Pb zircon dating and analysis of plate-tectonic setting (Saxo-Thuringian Zone, NE Bohemian massif, Germany). The Evolution of the Rheic Ocean: from Avalonian-Cadomian active margin to Alleghenian-Variscan collision. Geol. Soc. Am. Bull. 423, 61–96.
Linnemann, U., Pereira, F., Jeffries, T.E., Drost, K., Gerdes, A., 2008. The Cadomian Orogeny and the opening of the Rheic Ocean: the diacrony of geotectonic processes constrained by LA-ICP-MS U–Pb zircon dating (Ossa-Morena and Saxo-Thuringian Zones, Iberian and Bohemian Massifs). Tectonophysics 461, 21–43.
Linnemann, U., Ouzegane, K., Drareni, A., Hofmann, M., Becker, S., Gärtner, A., Sagawe, A., 2011. Sands of West Gondwana: an archive of secular magmatism and plate interactions—a case study from the Cambro-Ordovician section of the Tassili Ouan Ahaggar (Algerian Sahara) using U–Pb LA-ICP-MS detrital zircon ages. Lithos 123, 188–203.
Ludwig, K.R., 2012. Users Manual for Isoplot/Ex rev. 3.75. Berkeley Geochronology Center. Spec. Publ. 5, 1–75.
Ludwig, K.R., Mundil, R., 2002. Extracting reliable U–Pb ages and errors from complex populations of zircons from Phanerozoic tuffs. Geochim. Cosmochim. Acta 66, A463.
Manzotti, P., Poujol, M., Ballèvre, M., 2015. Detrital zircon in blueschist-facies metaconglomerates: implications for the Early Permian palaeotopography of the Western Alps. Int. J. Earth Sci. 104, 703–731.
Margalef, A., Castiñeiras, P., Casas, J.M., Navidad, M., Montserrat, L., Linnemann, U., Hofmann, M., Gärtner, A., 2017. Detrital zircons from the Ordovician rocks of the Pyrenees: geochronological constraints and provenance. Tectonophysics, http://dx.doi.org/10.1016/j.tecto.2016.03.015 (in press).
Mattauer, M., Laurent, P., Matte, P., 1996. Plissement Hercynien synschisteux postnappe et étirement subhorizontal dans le versant sud de la Montagne noire (sud du Massif central, France). C. R. Acad. Sci. Paris Ser. IIa 322, 309–315.
Meinhold, G., Morton, A.C., Avigad, D., 2013. New insights into peri-Gondwana paleogeography and the Gondwana super-fan system from detrital zircon U–Pb ages. Gondwana Res. 23, 661–665.
Meinhold, G., Morton, A.C., Fanning, C.M., Frei, D., Howard, J.P., Phillips, R.J., Strogen, D., Whitham, A.G., 2011. Evidence from detrital zircons for recycling of Mesoproterozoic and Neoproterozoic crust recorded in Paleozoic and Mesozoic sandstones of southern Libya. Earth Planet. Sci. Lett. 312, 164–175.
Melleton, J., Cocherie, A., Faure, M., Rossi, P., 2010. Precambrian protoliths and Early Paleozoic magmatism in the Massif Central: U–Pb data and the North Gondwana connection in the West European Variscan Belt. Gondwana Res. 17, 13–25.
Mezger, J.E., Gerdes, A., 2016. Early Variscan (Visean) granites int the core of central Pyrenean gneiss domes: implications from laser ablation U–Pb and Th-Pb studies. Gondwana Res. 29, 181–198.
Pereira, M.F., Chichorro, M., Solá, A.R., Silva, J.B., Sánchez-García, T., Bellido, F., 2011. Tracing the Cadomian magmatism with detrital/inherited zircon ages by in-situ U–Pb SHRIMP geochronology (Ossa-Morena Zone, SW Iberian Massif). Lithos 123, 204–217.
Pereira, M.F., Solá, A.R., Chichorro, M., Lope, L., Gerdes, A., Silva, J.B., 2012. North-Gondwana assembly, break-up and paleogeography: U–Pb isotope evidence from detrital and igneous zircons of Ediacaran and Cambrian rocks of SW Iberia. Gondwana Res. 22, 866–881.
Pitra, P., Poujol, M., Van Den Driessche, J., Poilvet, J.-C., Paquette, J.-L., 2012. Early Permian extensional shearing of an Ordovician granite: the Saint-Eutrope "C/S-like" orthogneiss (Montagne Noire, French Massif Central). C. R. Geoscience 344, 377–384.
Pouclet, A., Álvaro, J.J., Bardintzeff, J.-M., Gil Imaz, A., Monceret, E., Vizcaïno, D., 2017. Cambrian–Early Ordovician volcanism across the South Armorican and Occitan Domains of the Variscan Belt in France: continental break-up and rifting of the northern Gondwana margin. Geosci. Frontiers, http://dx.doi.org/10.1016/j.gsf.2016.03.002 (in press).
Poujol, M., Pitra, P., Van Den Driessche, J., Ruffet, G., Paquette, J.-L., Poilvet, J.-C., 2017. Two-stage partial melting during the Variscan extensional tectonics (Montagne Noire, France). Int. J. Earth Sci., http://dx.doi.org/10.1007/s00531-016-1369-1 (in press).
Raumer (von), J.F., Stampfli, G.M., 2008. The birth of the Rheic Ocean — Early Palaeozoic subsidence patterns and subsequent tectonic plate scenarios. Tectonophysics 461, 9–20.
Roger, F., Respault, J.-P., Brunel, M., Matte, P., Paquette, J.-L., 2004. Première datation U–Pb des orthogneiss œillés de la zone axiale de la Montagne noire (Sud du Massif central) : nouveaux témoins du magmatisme ordovicien dans la chaîne varisque. C. R. Geoscience 336, 19–28.
Rubio-Ordóñez, A., Gutiérrez-Alonso, G., Valverde-Vaquero, P., Cuesta, A., Gallastegui, G., Gerdes, A., Cárdenes, V., 2015. Arc-related Ediacaran magmatism along the northern margin of Gondwana: geochronology and isotopic geochemistry from northern Iberia. Gondwana Res. 27, 216–227.
Sambridge, M.S., Compston, W., 1994. Mixture modelling of multi-component data sets with application to ion-probe zircon ages. Earth Planet. Sci. Lett. 128, 373–390.

Please cite this article in press as: Padel M, et al. U–Pb laser ablation ICP-MS zircon dating across the Ediacaran–Cambrian transition of the Montagne Noire, southern France. C. R. Geoscience (2017), http://dx.doi.org/10.1016/j.crte.2016.11.002

Sláma, J., Košler, J., 2012. Effects of sampling and mineral separation on accuracy of detrital zircon studies. Geochem. Geophys. Geosyst. 13, 1–17.

Sláma, J., Košler, J., Condon, D.J., Crowley, J.L., Gerdes, A., Hanchar, J.M., Horstwood, M.S.A., Morris, G.A., Nasdala, L., Norberg, N., Schaltegger, U., Schoene, B., Tubrett, M.N., Whitehouse, M.J., 2008. Plešovice zircon — a new natural reference material for U–Pb and Hf isotopic microanalysis. Chem. Geol. 249, 1–35.

Soula, J.-C., Debat, P., Brusset, S., Bessière, G., Christophoul, F., Deramond, J., 2001. Thrust-related, diapiric and extensional doming in a frontal orogenic wedge: example of the Montagne Noire, southern French Hercynian belt. J. Struct. Geol. 23, 1677–1699.

Squire, R.J., Campbell, I.H., Allen, C.M., Wilson, C.J.L., 2006. Did the Transgondwana Supermontin trigger the explosive radiation of animals on Earth? Earth Planet. Sci. Lett. 250, 116–133.

Tack, L., Wingate, M.T.D., De Waele, B., Meert, J., Belousova, E., Griffin, B., Tahon, A., Fernandez-Alonso, M.A., 2010. The 1375 Ma "Kibaran event" in central Africa: prominent emplacement of bimodal magmatism under extensional regime. Precambr. Res. 180, 63–84.

Tack, L., Wingate, M.T.D., Liégeois, J.P., Fernández-Alonso, M., Deblond, A., 2001. An Early Neoproterozoic magmatism (1000–1910 Ma) of the Zadinian and Mayumbian Groups (Bas-Congo): onset of Rodinia rifting at the western edge of the Congo craton. Precambr. Res. 110, 277–306.

Talavera, C., Montero, P., Martínez Poyatos, D., Williams, I.S., 2012. Ediacaran to Lower Ordovician age for rocks ascribed to the Schist-Graywacke Complex (Iberian Massif, Spain): evidence from detrital zircon SHRIMP U–Pb geochronology. Gondwana Res. 22, 928–942.

Van Achterbergh, E., Ryan, C.G., Jackson, S.E., Griffin, W.L., 2001. Data reduction software for LA-ICP-MS: appendix. In: Sylvester, P.J. (Ed.), Laser Ablation-ICP-mass spectrometry in the Earth Sciences: principles and applications. MAC Short Courses Series, Ottawa, Ontario, Canada, pp. 239–243.

Van Den Driessche, J., Brun, J.-P., 1992. Tectonic evolution of the Montagne Noire (French Massif Central): a model of extensional dome. Geodin. Acta 5, 85–99.

Vermeesch, P., 2004. How many grains are needed for a provenance study? Earth Planet. Sci. Lett. 224, 351–441.

Williams, I.S., Fiannacca, P., Cirrincione, R., Pezzino, A., 2012. Peri-Gondwanan origin and early geodynamic history of NE Sicily: a zircon tale from the basement of the Peloritani Mountains. Gondwana Res. 22, 855–865.

Please cite this article in press as: Padel M, et al. U–Pb laser ablation ICP-MS zircon dating across the Ediacaran–Cambrian transition of the Montagne Noire, southern France. C. R. Geoscience (2017), http://dx.doi.org/10.1016/j.crte.2016.11.002